J. Fluid Mech. (1993), *vol.* 249, *pp.* 99–120

Analysis of thermal ignition in supersonic flat-plate boundary layers

By H. G. IM, J. K. BECHTOLD AND C. K. LAW

Department of Mechanical and Aerospace Engineering, Princeton University, Princeton, NJ 08544, USA

(Received 12 June 1992 and in revised form 14 October 1992)

The ignition of the supersonic boundary layer flow of a combustible mixture over a flat plate is studied through both direct numerical integration and activation energy asymptotics. Since ignition can be induced through either internally generated viscous heating or heat transfer from a hot wall, analyses are conducted for both an adiabatic wall and an isothermal wall whose temperature can be either higher or lower than the maximum frozen temperature in the flow. The analyses provide a description of the flow structure under various ignition situations, especially the extent of flow non-similarity and the interaction between the inner reaction region and the outer frozen regions. Explicit expressions for the ignition distance are obtained for all ignition situations, and the corresponding effects of the physical parameters on the ignition delay are also assessed. Specifically, it is demonstrated that, for low free-stream Mach number M_∞, the ignition distance increases linearly with M_∞ because of the decreased residence time, and for high M_∞ it decreases exponentially with M_∞ because of viscous heating. Results from the asymptotic analyses are found to compare well with those obtained from the direct numerical integration.

1. Introduction

The development of the scramjet engine for supersonic propulsion (Waltrup 1986; Law 1992) and the scramaccelerator for hypervelocity projectile launching (Humphrey & Sobota 1991) has renewed interest in supersonic combustion. In contrast to subsonic situations, high-speed flows generate a considerable amount of heat through viscous dissipation, which can play an essential role in such practical issues as ignition delay and flame stabilization in supersonic propulsion, and premature ignition in scramaccelerators. The relevant fundamental combustion phenomenon here is the ignition within chemically reactive supersonic boundary layer flows.

A large number of theoretical studies have been performed on ignition in subsonic laminar boundary layer flows. Since the presence of finite-rate chemical reaction can introduce an additional timescale to an otherwise similar boundary layer flow, chemically reacting boundary layer flows are frequently non-similar. Consequently, many of the theoretical studies were concerned with the issue of non-similarity. These include the series expansion technique of Marble & Adamson (1954) and Cheng & Kovitz (1957, 1958) and the iteration technique of Dooley (1957) for the mixing layer flow, the numerical solution of Sharma & Sirignano (1970) for several types of boundary layer flows, and the activation energy asymptotic analysis of Law & Law (1979) for the isothermal flat-plate boundary layer. In the last study the weakly

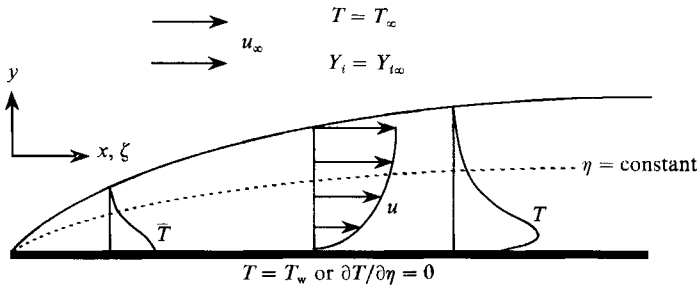

FIGURE 1. Schematic of the model illustrating boundary layer flow over a flat plate.

reactive flow was shown to be locally similar in the limit of large activation energy, and an explicit expression for the ignition distance was consequently derived. Recently, Treviño & Méndez (1991) included complex chemistry in an asymptotic analysis of the flat-plate boundary layer flow of a hydrogen/air mixture. A common result in each of the above studies is that the ignition distance basically scales linearly with the free-stream velocity.

A straightforward application of the above subsonic scaling on the ignition distance to supersonic flows would show that boundary-layer flame stabilization in supersonic combustors requires excessively long ignition distances and therefore is not a viable concept. This assessment, however, does not take into account the fact that a high-speed flow also possesses a tremendous amount of kinetic energy which, when converted into thermal energy through viscous heating in the boundary layer, constitutes an additional source for ignition. Thus the ignition distance could conceivably be shortened when viscous heating is accounted for. Indeed, viscous heating is the only heat source to induce ignition in an adiabatic system.

The effect of viscous heating on ignition was first considered by Jackson & Hussaini (1988) in their asymptotic study of a supersonic mixing layer. Ju & Niioka (1991) examined a similar problem with multi-step chemistry and $O(1)$ temperature difference between the two free streams. In both of these studies, the two streams were assumed to be at nearly the same velocity, and thus viscous heating was a higher-order effect. Grosch & Jackson (1991) performed a numerical and asymptotic analysis of the mixing-layer ignition problem, in which they allowed for $O(1)$ differences in free-stream temperatures and velocities. Their results illustrate the full effect of viscous heating on ignition and they provide ignition criteria for various values of system parameters. More recently, Figueira da Silva, Deshaies & Champion (1992) also assessed the role of $O(1)$ viscous heating effects in their numerical study of supersonic flat-plate boundary-layer ignition with detailed hydrogen/air chemistry.

In the present paper we shall perform a comprehensive numerical and asymptotic study of the weakly reactive laminar supersonic flat-plate boundary layer flow with $O(1)$ viscous heating and simplified, one-step overall reaction, up to the state of ignition. We are interested in identifying the structure of the boundary layer flow under all possible heating and ignition situations, and consequently determining explicit expressions for the associated ignition distance in terms of all relevant parameters. Specifically, we shall show that there are three distinctively different ignition situations, namely when the wall is: (i) adiabatic such that viscous heating is the only ignition source, (ii) isothermal and subadiabatic (heat is transferred to the gas) in the inert limit, and (iii) isothermal and superadiabatic (heat is transferred

from the gas) in the inert limit. It is reasonable to anticipate that external heating from the wall is the dominant source for ignition in the second case and is therefore relevant for relatively low Mach number flows, while in the first and third cases viscous heating is the dominant source for ignition and therefore they are relevant for high Mach number flows. Additional issues of interest in the present study are the extent of non-similarity and local-similarity for the various ignition regimes, and the definitions of ignition based on either the steady-state, turning-point consideration or the non-steady, thermal explosion consideration.

In the next section the mathematical problem will be formulated. In §3 we present numerical solutions for the full problem as well as those obtained by assuming local-similarity in the flow field. In §4 we present the asymptotic analysis for both adiabatic and isothermal walls, and explicit expressions for the ignition distances are derived. Finally, in §5 we summarize our results and add further discussions.

2. Formulation

As shown in figure 1, we consider a laminar boundary layer flow of a combustible mixture with supersonic free-stream velocity u_∞, temperature $\hat{T}_\infty$, density ρ_∞, pressure $\hat{p}$ and species mass fractions $\hat{Y}_{i,\infty}$ over an impermeable, non-catalytic flat plate. Both adiabatic and isothermal walls are considered in our analysis. By restricting the ignition phenomena to be thermally induced, it is adequate to represent the reaction mechanism as a one-step overall irreversible reaction

$$\nu_{\mathrm{O}}[\mathrm{O}]+\nu_{\mathrm{F}}[\mathrm{F}]\rightarrow\nu_{\mathrm{P}}[\mathrm{P}] \tag{1}$$

between the fuel F and oxidant O to form a product P, with an Arrhenius reaction rate proportional to

$$\rho^{p+q}\hat{Y}_{\mathrm{O}}^{p}\,\hat{Y}_{\mathrm{F}}^{q}\,\hat{T}^{r}\exp\left(-E_{\mathrm{a}}/R^{0}\hat{T}\right). \tag{2}$$

Here ν_{O} and ν_{F} are the stoichiometric coefficients, E_{a} is the activation energy, R^0 the gas constant, and $\hat{T}$ the temperature. For simplicity, we adopt Chapman's linear viscosity law such that $\rho\hat{\mu}$ becomes constant in the current isobaric situation. We further assume constant properties such as specific heat c_p, density-weighted mass diffusion coefficients $\rho^2 D_i$, and unity values for the Lewis and Prandtl numbers. Although not presented here, we have performed numerical studies with arbitrary Lewis number and found that these effects play a secondary role in the ignition process.

In terms of non-dimensional quantities, the conservation equations for momentum, mass fraction of species i, and static energy in the supersonic boundary layer are (see, for example, Chung 1965; Williams 1985)

$$f'''+ff''=0, \tag{3}$$

$$\frac{\partial^2 Y_i}{\partial\eta^2}+f\frac{\partial Y_i}{\partial\eta}-2\zeta f'\frac{\partial Y_i}{\partial\zeta}=\zeta Y_{\mathrm{O}}^{p}\,Y_{\mathrm{F}}^{q}\,T^{r-p-q+1}\exp\left(-T_{\mathrm{a}}/T\right), \tag{4}$$

$$\frac{\partial^2 T}{\partial\eta^2}+f\frac{\partial T}{\partial\eta}-2\zeta f'\frac{\partial T}{\partial\zeta}=-\zeta Y_{\mathrm{O}}^{p}\,Y_{\mathrm{F}}^{q}\,T^{r-p-q+1}\exp\left(-T_{\mathrm{a}}/T\right)-2\mu[f''(\eta)]^2, \tag{5}$$

which are supplemented by the ideal-gas equation of state, and in these equations a prime denotes $\mathrm{d}/\mathrm{d}\eta$ and $\mu\equiv\frac{1}{2}(\gamma-1)M_\infty^2\,T_\infty$. The non-dimensional temperature, T,

and the mass fraction for species i, Y_i, are given in terms of the original variables by $T = c_p \hat{T}/Q\hat{Y}_{F\infty}$ and $Y_i = \hat{Y}_i/\sigma_i \hat{Y}_{F\infty}$, where Q is the heat of reaction per unit mass of fuel and σ_i is the stoichiometric oxidizer-to-fuel mass ratio such that $\sigma_F = 1$. The parameters appearing in these equations include the ratio of specific heats $\gamma = c_p/c_v$, the non-dimensional activation temperature $T_a = c_p(E_a/R^0)/Q\hat{Y}_{F\infty}$, and the free-stream Mach number $M_\infty = u_\infty/(\gamma R^0 \hat{T}_\infty/\bar{W})^{\frac{1}{2}}$. The variables ζ and η are normalized Howarth–Dorodnitsyn variables defined as

$$\eta = \left(\frac{u_\infty}{2\rho_\infty \hat{\mu}_\infty x}\right)^{\frac{1}{2}} \int_0^y \rho(x, y')\, dy', \tag{6}$$

$$\zeta = x\left(\frac{2B\nu_F W_F}{u_\infty W_O^p W_F^q}\right)\left(\frac{\hat{p}\bar{W}}{R^0}\right)^{p+q-1} \sigma_O^p \hat{Y}_{F\infty}^r \left(\frac{Q}{c_p}\right)^{r-p-q+1}, \tag{7}$$

and f is the stream function $\psi(x, y)$ normalized as

$$f(\eta) = \psi(x, y)/(2\rho_\infty \hat{\mu}_\infty u_\infty x)^{\frac{1}{2}}. \tag{8}$$

The variable ζ can be interpreted as a reduced Damköhler number, representing the ratio of a characteristic flow time to a characteristic reaction time. In these expressions, B is the frequency factor of the chemical reaction, W_i the molecular weights, $\bar{W}$ the average molecular weight, and x and y the physical coordinates parallel and normal to the surface of the plate. The last term in the energy equation (5) accounts for the viscous heating, which represents the amount of kinetic energy that is converted to thermal energy as the flow is slowed down near the wall. For supersonic boundary layer flows, this heat source term plays an important role in the attainment of ignition.

The above equations (3)–(5) are to be solved subject to the following boundary conditions:

$$f(0) = f'(0) = 0, \quad f'(\infty) = 1, \tag{9}$$

$$(\partial Y_i/\partial\eta)(0, \zeta) = 0, \quad Y_i(\infty, \zeta) = Y_{i\infty}, \tag{10}$$

$$T(\infty, \zeta) = T_\infty, \tag{11}$$

$$(\partial T/\partial\eta)(0, \zeta) = 0 \text{ for adiabatic wall}, \tag{12a}$$

$$T(0, \zeta) = T_w \text{ for isothermal wall}. \tag{12b}$$

Equations (3) and (9) are the self-similar Blasius equations for boundary layer flows over a flat plate, and their solutions are well known (Schlichting 1979). These equations are decoupled from the transport equations for the scalar quantities T and Y_i, and we can therefore study the effect of this flow field on the ignition characteristics of supersonic boundary layers.

We will restrict our study to weakly reactive states through which ignition evolves from an initially frozen state. Then the inert solution provides the *initial* condition at the leading edge for the numerical calculation and also represents the leading-order, basic temperature and concentration profiles for the asymptotic analysis. In the frozen state, the flow is self-similar and the energy equation (5) becomes

$$\frac{\partial^2 T_f}{\partial\eta^2} + f\frac{\partial T_f}{\partial\eta} = -2\mu[f''(\eta)]^2, \tag{13}$$

where the subscript f denotes the frozen solution.

It is convenient to make the convection-free coordinate transformation $\xi = f'(\eta)$ such that $0 \leqslant \xi \leqslant 1$ (Law & Law 1979), which will serve as the transverse independent variable, so that (13) takes the simplified form

$$\partial^2 T_f / \partial \xi^2 = -2\mu. \tag{14}$$

This has the solution $T_f = c_1 + c_2 \xi - \mu \xi^2$, where the constants c_1 and c_2 are to be determined by applying (11) together with either (12*a*) or (12*b*).

For the adiabatic wall, application of boundary conditions (11) and (12*a*) yields the frozen solution

$$T_f = T_\infty + \mu - \mu \xi^2, \tag{15}$$

which achieves a maximum value of $T_c = T_\infty + \mu$ at $\xi = 0$. For combustion systems with large activation energies, the reaction term is very sensitive to temperature variations and thus it is reasonable to expect that ignition will occur near the wall.

For the isothermal wall, application of boundary conditions (11) and (12*b*) yields the solution

$$T_f = T_w - \alpha \xi - \mu \xi^2, \tag{16}$$

where $\alpha \equiv \beta - \mu = (T_w - T_\infty) - \mu$ represents the difference between the inviscid heat transfer parameter, β, and the viscous heating term, μ. If $\alpha > 0$, the frozen temperature profile (16) achieves a maximum value of $T_c = T_w$ at $\xi = 0$ and, as for the adiabatic wall case, we expect that ignition will occur near the wall. In this situation, heat conduction from the hot wall dominates viscous heating and it is therefore the primary energy source causing ignition.

Next consider $\alpha < 0$ for the isothermal wall problem, so that viscous heating is dominant. The temperature profile (16) now has a maximum value of $T_c = T_w + \alpha^2/4\mu$ at $\xi = -\alpha/2\mu > 0$, and thus ignition will occur at some finite distance away from the wall. Unlike the $\alpha > 0$ case, heat transfer is now toward the wall. Because the point of maximum temperature lies in the interior of the boundary layer, it loses heat to the frozen regions on either side.

Each of the three solutions discussed above represents a frozen state. In the presence of finite-rate reaction, the flow is weakly reactive and, through the nonlinear Arrhenius kinetics, will eventually attain a state of thermal runaway. We shall first discuss the ignition dynamics for these three cases through the numerical solution of the full system (4)–(5) and (10)–(12). We shall then perform an asymptotic analysis of these situations and derive explicit expressions for the ignition distances expressed as functions of all the relevant physical parameters of the problem.

3. Numerical solutions

Equations (4)–(5) and (10)–(12) are solved using a second-order finite-difference scheme with implicit determination in the η-direction and marching along the streamwise coordinate ζ, where the step size is readjusted as the solution approaches the ignition point in order to capture the abrupt temperature rise. For simplicity we have assumed $p = q = r = 1$ and that the mixture is stoichiometric, with $Y_{F\infty} = Y_{O\infty} = 1$. We have used the parameter values $Q = 1.0 \times 10^4$ kcal kg^{-1}, $c_p = 0.25$ kcal kg^{-1} K^{-1}, $E_a = 60$ kcal/mole and $\gamma = 1.4$, which are typical numbers for hydrocarbon/air mixtures.

The streamwise variation of the temperature profile within the boundary layer in the $\xi = f'(\eta)$ coordinate is shown in figure 2(*a–c*) for the three ignition situations,

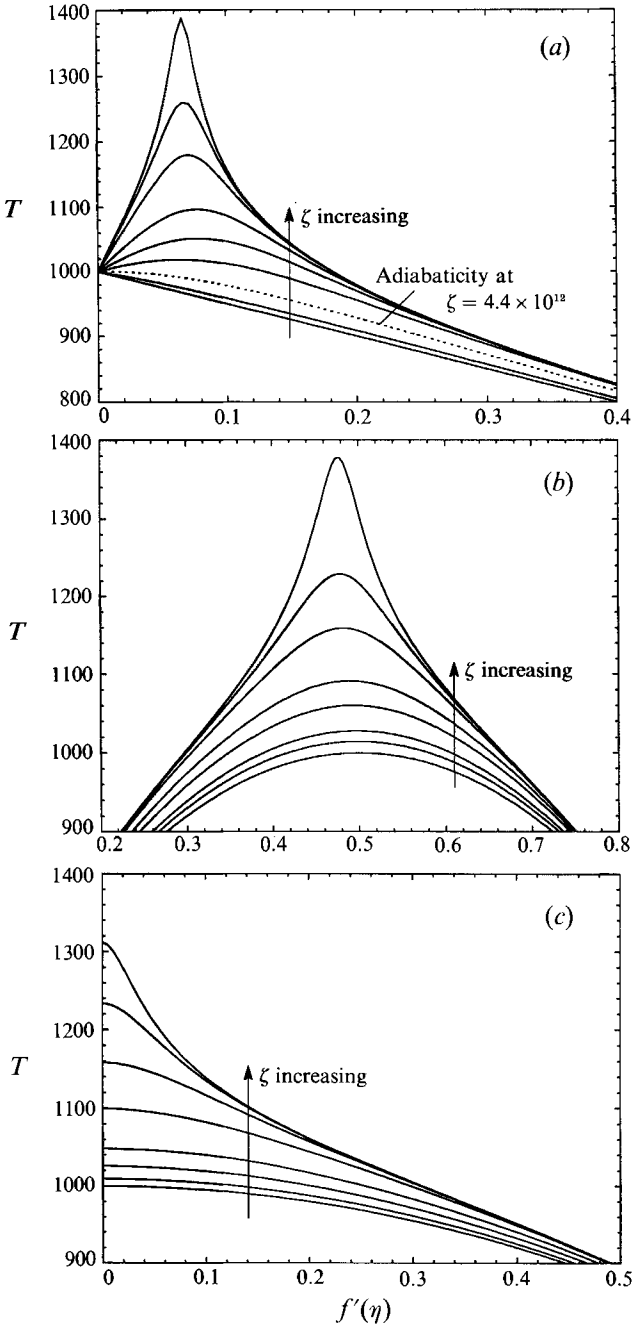

FIGURE 2. Evolution of the temperature profiles as computed numerically. (*a*) The subadiabatic wall case with $\hat{T}_\infty = 500$ K, $\hat{T}_w = 1000$ K, $M_\infty = 0$, $\zeta = 0$, 2.0, 4.4, 5.1641, 5.2242, 5.2366, 5.2395, 5.2398, 5.2399 ($\times 10^{12}$). (*b*) The superadiabatic wall case with $\hat{T}_\infty = \hat{T}_w = 500$ K, $M_\infty = 4.472$, $\zeta = 0$, 2.0, 3.0, 4.0, 4.2872, 4.4394, 4.4658, 4.4734 ($\times 10^{11}$). (*c*) The adiabatic wall case with $\hat{T}_\infty = 500$ K, $M_\infty = 2.236$, $\zeta = 0$, 0.5, 1.0, 1.3, 1.4565, 1.4768, 1.4798, 1.4801 ($\times 10^{11}$).

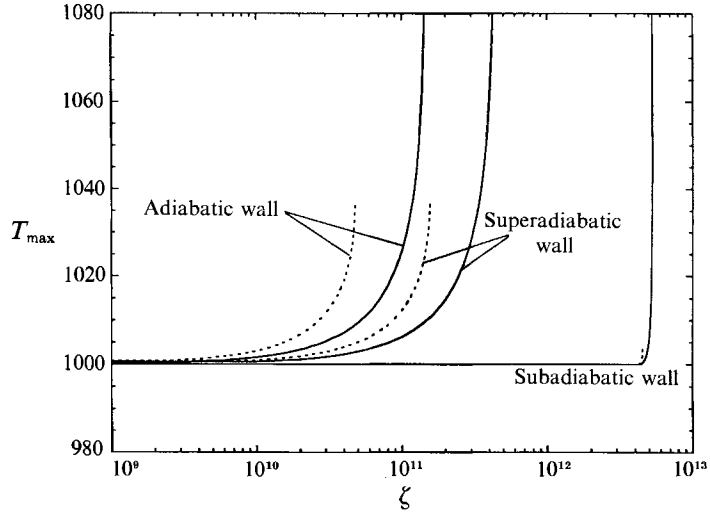

FIGURE 3. Streamwise variation of the maximum temperature for the cases in figure 2: ——, full numerical solution with non-similar terms; ---, numerical solution with local-similarity assumption.

where the parameters are chosen such that the maximum value of the inert temperature profile is the same in each case. The ambient temperature is chosen to be $\hat{T}_\infty = 500$ K while the profile at the leading edge, $\zeta = 0$, is taken to be the similar frozen solution in each case. It is seen that the temperature increases with increasing ζ as reaction progresses. For the isothermal wall with $\alpha > 0$, the heat required for ignition is supplied mainly from the hot wall, and in figure 2(*a*) we have plotted the temperature evolution for the case of zero viscous heating ($\mu = 0$), which is identical to the problem of boundary-layer ignition in subsonic flows considered by Law & Law (1979). It is seen that the temperature gradient at the wall vanishes at $\zeta \approx 4.4 \times 10^{12}$, while thermal runaway occurs further downstream at $\zeta \approx 5.24 \times 10^{12}$, as indicated by the dramatic increase in the temperature bulge over relatively short distances. We remark that, owing to the temperature sensitivity of the reaction rate, the point at which the wall is adiabatic becomes closer to the location of the temperature blow-up as the activation energy is increased.

Figures 2(*b*) and 2(*c*) respectively show the evolution of temperature profiles for the isothermal wall with $\alpha < 0$, and the adiabatic wall. In particular, figure 2(*b*) corresponds to the extreme case of a cold wall, $T_w = T_\infty$, such that the energy for ignition is acquired solely from viscous heating. Although there does not exist a critical point where the wall passes through adiabaticity in these two cases, there is nevertheless an ignition delay, and the points at which the temperature profiles blow up are given by $\zeta \approx 4.47 \times 10^{11}$ and $\zeta \approx 1.48 \times 10^{11}$, respectively.

The streamwise history of the maximum temperature for each case is plotted in figure 3 as a solid curve, which clearly illustrates the existence of a critical ignition distance, ζ_I, at which thermal runaway occurs. It may be noted that since wall temperatures and free-stream velocities are different for the three cases, it is not appropriate to compare their relative distances to achieve ignition.

Since we are only interested in the weakly reactive solutions up to the state of ignition, we have also explored the accuracy of approximating the temperature and species profiles as being locally similar by neglecting the $\partial/\partial\zeta$ terms in (4) and (5), so that the coordinate ζ now appears only parametrically in the reaction rate term. The

maximum temperature variation with ζ for these locally similar solutions is plotted in figure 3 as dotted lines. For all three cases, a critical value of ζ was found beyond which we were unable to converge to a solution, which suggests that these solution curves posses turning points. These results demonstrate the two types of problems that can arise in the ignition analyses, as discussed in Liñán & Crespo (1976), if we regard the transverse convective term in our equations as playing the role of a time derivative. That is, similar or locally similar solutions can be interpreted as steady-state solutions for which it is known that turning point behaviour exists. By accounting for the non-similar convective term, we are considering the full evolutionary problem that exhibits thermal runaway.

Our results show that the locally similar approximation underestimates the actual ignition distance, determined by solving the full non-similar equations, by a factor of about two for the adiabatic wall and the superadiabatic isothermal wall cases. This indicates that streamwise convective transport is an efficient means of sweeping away heat liberated by the chemical reaction. The distinction between the similar and non-similar solutions becomes relatively indiscernible for the hot wall case (see figure 3). It will be shown in §4 that the ignition characteristics for this case are primarily determined by the locally similar reactive–diffusive equations in a narrow region adjacent to the hot wall. To leading order, there is no interaction between the solution in this reaction zone and the non-similar frozen solution in the outer region away from the wall. Thus, the inclusion of non-similar effects will only lead to a higher-order correction to the ignition distance, and the solution obtained by making the local-similarity assumption is accurate to first approximation for the hot wall ignition case. The local-similarity assumption was also found to be appropriate for studies regarding ignition of initially separated reactants (Liñán & Crespo 1976), and ignition in subsonic boundary layers (Law & Law 1979).

In addition to the sample calculation reported above, we have computed the ignition distance for several other values of the parameters β and μ, and these results will be compared to the results of the asymptotic analysis to be presented in the next section.

4. Asymptotic analysis

In this section we exploit the fact that the activation energy is large in order to derive explicit formulae for the ignition distance. In particular, we will construct asymptotic solutions in inverse powers of the activation energy to show how temperature perturbations to the frozen state can give rise to ignition. The expansion parameter is defined as $\epsilon = T_c^2/T_a$, where T_c represents the maximum temperature for the inert profiles discussed in §2. Again using $\xi = f'(\eta)$ as the independent transverse variable, our governing equations (5), (11) and (12) become

$$\frac{\partial^2 T}{\partial \xi^2} - \frac{2\xi\zeta}{[f''(\eta)]^2}\frac{\partial T}{\partial \zeta} = -\frac{\zeta Y_O^p Y_F^q T^{r-p-q+1}}{[f''(\eta)]^2}\exp(-T_a/T) - 2\mu, \tag{17}$$

$$T(1,\zeta) = T_\infty, \quad T(\xi,0) = T_f(\xi), \tag{18}$$

$$(\partial T/\partial \xi)(0,\zeta) = 0 \text{ for adiabatic wall}, \tag{19a}$$

$$T(0,\zeta) = T_w \text{ for isothermal wall}. \tag{19b}$$

In this analysis, reaction is sufficiently weak so that reactant consumption is negligible to a first approximation. Therefore, the species equations decouple from

the energy equation, and Y_O and Y_F in (17) are replaced by their constant free-stream values to leading order. We will now construct solutions to this system in order to calculate the minimum ignition distance for both adiabatic and isothermal walls.

4.1. *Adiabatic wall*

In the limit $T_a \to \infty$, the reaction rate term is absent in (17) and as shown in §2 the frozen temperature profile has the self-similar form

$$T_f(\xi) = T_c - \mu\xi^2, \tag{20}$$

where $T_c = T_\infty + \mu$. To consider large but finite values of T_a, we introduce the small expansion parameter $\epsilon = T_c^2/T_a \ll 1$, where T_c is seen to vary with the square of the Mach number. Because the Damköhler number is typically very large, the reaction rate term is extremely sensitive to temperature variations and a temperature rise of $O(\epsilon)$ is sufficient for ignition to occur. Furthermore, the reaction will initiate in a thin zone near the hottest location in the frozen flow field. For the present case, this reaction zone will be near $\xi = 0$, and the parabolic shape of the frozen profile (20) suggests that this inner structure is of $O(\epsilon^{\frac{1}{2}})$ thickness. To examine this structure, we introduce the inner stretched variable

$$\chi = \mu^{\frac{1}{2}}\xi/\epsilon^{\frac{1}{2}}, \tag{21}$$

and seek an inner solution of the form

$$T_{in}(\chi, \zeta) = T_f(\chi) + \epsilon\theta_0(\chi, \zeta) + \epsilon^{\frac{3}{2}}\theta_1(\chi, \zeta) + O(\epsilon^2), \tag{22}$$

while $f''(\eta)$ is also expanded as

$$f''(\eta) = f''(0) + o(\epsilon). \tag{23}$$

When (22) and (23) are inserted into (17) and (19*a*) and the first two terms in our perturbation expansion are retained, we obtain

$$\frac{\partial^2}{\partial\chi^2}(\theta_0 + \epsilon^{\frac{1}{2}}\theta_1) - \epsilon^{\frac{3}{2}}\frac{2\chi\zeta}{\mu^{\frac{3}{2}}[f''(0)]^2}\frac{\partial}{\partial\zeta}(\theta_0 + \epsilon^{\frac{1}{2}}\theta_1) = -\Delta_{aw}[1 + O(\epsilon^{\frac{1}{2}})]\exp(\theta_0 - \chi^2), \tag{24}$$

$$\frac{\partial\theta_0}{\partial\chi} = \frac{\partial\theta_1}{\partial\chi} = 0 \quad \text{at} \quad \chi = 0, \tag{25}$$

where Δ_{aw} is the reduced Damköhler number expressed as

$$\Delta_{aw} = \frac{\zeta}{\mu[f''(0)]^2} Y_{O\infty}^p T_c^{r-p-q+1} \exp(-T_a/T_c), \tag{26}$$

which is at most algebraically small in ϵ. In addition to satisfying the boundary conditions (25), solutions to (24) must also match appropriately to the outer frozen solutions at $\chi \to \infty$.

We note that the convective term in (24) is of smaller magnitude than the diffusion term. Thus, in this region there appears to be an order of magnitude balance between transverse diffusion and reaction. However, if we assume that $\Delta_{aw} = O(1)$, then we arrive at a contradiction as no solution can be found that satisfies the boundary and matching conditions. This suggests that we have overestimated the magnitude of the ignition distance, or equivalently the Damköhler number. Therefore, effects due to reaction are of yet higher order, and it is appropriate to rescale Δ_{aw} as

$$\Delta_{aw} = \epsilon^{\frac{1}{2}}\tilde{\Delta}_{aw} \tag{27}$$

so that, to the first two orders, the structure equations become

$$\partial^2\theta_0/\partial\chi^2 = 0, \tag{28}$$

$$\partial^2\theta_1/\partial\chi^2 = -\tilde{\Delta}_{\rm aw}\exp(\theta_0-\chi^2), \tag{29}$$

to be solved subject to

$$\partial\theta_0/\partial\chi = \partial\theta_1/\partial\chi = 0 \quad \text{at} \quad \chi = 0. \tag{30}$$

Integration of (28) subject to the boundary condition (30) reveals that θ_0 is a function of ζ only, and thus (29) can be readily integrated once to yield

$$\frac{\partial\theta_1}{\partial\chi} = -\tilde{\Delta}_{\rm aw}\exp[\theta_0(\zeta)]\int_0^{\chi}\exp(-y^2)\,{\rm d}y, \tag{31}$$

from which it follows that

$$(\partial\theta_1/\partial\chi)(\infty,\zeta) = -\tfrac{1}{2}\pi^{\frac{1}{2}}\tilde{\Delta}_{\rm aw}\exp[\theta_0(\zeta)]. \tag{32}$$

Equation (32) now provides us with a boundary condition for the outer solution at $\xi = 0$ through matching.

In the frozen region away from the reaction zone boundary layer we seek solutions of the form $T_{\rm out}(\xi,\zeta) = T_{\rm f}(\xi)+\epsilon\Phi_0(\xi,\zeta)+O(\epsilon^{\frac{3}{2}})$, and by inserting this into (17) and (18) we obtain at leading order

$$\frac{\partial^2\Phi_0}{\partial\xi^2} - \frac{2\xi}{[f''(\eta)]^2}\zeta\frac{\partial\Phi_0}{\partial\zeta} = 0, \tag{33}$$

$$\Phi_0(\xi,0) = 0, \quad \Phi_0(1,\zeta) = 0. \tag{34}$$

We remark that an $O(\epsilon^{\frac{1}{2}})$ temperature perturbation term to the frozen solution in this outer region can be shown to possess only the trivial solution. This outer region is non-similar as a balance between transverse diffusion and streamwise convection is maintained. The additional boundary condition needed to solve this system is obtained by matching to the inner solution, which yields

$$\begin{aligned}\Phi_0(0,\zeta) &= \theta_0(\zeta),\\ (\partial\Phi_0/\partial\xi)(0,\zeta) &= \mu^{\frac{1}{2}}(\partial\theta_1/\partial\chi)(\infty,\zeta),\end{aligned} \tag{35}$$

and (32) can be used to reduce this to

$$\partial\Phi_0/\partial\xi = -\tfrac{1}{2}(\pi\mu)^{\frac{1}{2}}\tilde{\Delta}_{\rm aw}\exp[\Phi_0(0,\zeta)]. \tag{36}$$

Finally, noting that $\tilde{\Delta}_{\rm aw}$ varies linearly with ζ, we can eliminate all of the parameters in this outer problem by introducing the coordinate translation $\sigma = \ln[\frac{1}{2}(\pi\mu)^{\frac{1}{2}}\tilde{\Delta}_{\rm aw}]$ so that our system takes the form

$$\frac{\partial^2\Phi_0}{\partial\xi^2} - \frac{2\xi}{[f''(\eta)]^2}\frac{\partial\Phi_0}{\partial\sigma} = 0, \tag{37}$$

$$\Phi_0(\xi,-\infty) = \Phi_0(1,\sigma) = 0, \tag{38}$$

$$(\partial\Phi_0/\partial\xi)(0,\sigma) = -\exp[\Phi_0(0,\sigma)+\sigma]. \tag{39}$$

The system (37)–(39) is similar to that derived by Liñán & Williams (1971) for the problem of ignition of a reactive solid, except for the appearance of a non-constant coefficient in our differential operator. We have numerically solved this system and figure 4 shows the variation of the maximum temperature perturbation $\Phi_0(0,\sigma)$ with

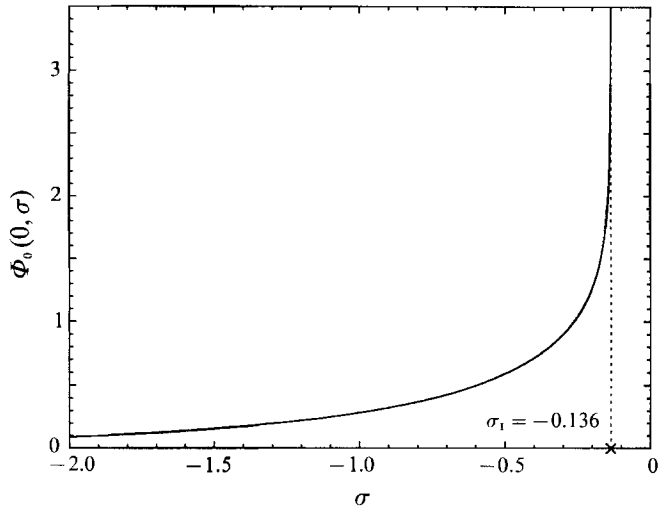

FIGURE 4. Solution of (37)–(39) for the maximum perturbed temperature $\Phi_0(0,\sigma)$ versus σ in the adiabatic wall problem.

the *time* variable σ. It is found that $\Phi_0(0,\sigma)$ blows up at $\sigma = \sigma_I \approx -0.136$, which can be regarded as the ignition time, and therefore, using the definitions of σ and $\tilde{\Delta}_{aw}$ we obtain the following expression for the ignition distance, ζ_I:

$$\zeta_I = 2\exp(\sigma_I)\left(\frac{\mu\epsilon}{\pi}\right)^{\frac{1}{2}} \frac{[f''(0)]^2}{Y_{O\infty}^{p} T_c^{r-p-q+1}} \exp(T_a/T_c), \tag{40}$$

where $f''(0) \approx 0.4696$.

To summarize, the above analysis has revealed that the structure of weakly reactive boundary layer flow over an adiabatic wall consists of an inner locally similar reactive–diffusive zone next to the wall, and an outer non-similar convective–diffusive zone. Since the system (37)–(39) is parameter-free, it needs to be numerically solved only once in order to obtain the universal result (40) for the ignition distance. This represents a significant simplification over the original system (17)–(19).

If we attempt to simplify matters further by assuming a locally similar outer flow field by neglecting the second term in (37), then an implicit expression for the maximum temperature perturbation $\Phi_0(0,\sigma)$ as a function of σ can easily be found, namely

$$\sigma = -\Phi_0(0,\sigma) + \ln \Phi_0(0,\sigma). \tag{41}$$

In accord with our earlier discussions, this locally similar result exhibits turning-point behaviour and the critical ignition point, evaluated by setting $d\sigma/d\Phi_0 = 0$, is found to be $\sigma_I = -1$. When this value is inserted into (40) we find that the local-similarity assumption leads to an underestimation of the ignition distance by $\exp(-0.136+1) \approx 2.37$, which is consistent with the numerical results in §3.

From a practical standpoint, it is useful to discuss how the actual ignition distance in terms of the original physical coordinate, x_I, varies with the physical parameters in the problem. In particular, it follows from (7) that ζ_I must be *multiplied* by a factor of u_∞, or equivalently M_∞, to observe the dependence of x_I on Mach number. Thus, in figure 5 we plot the quantity $M_\infty \zeta_I$ versus M_∞ as determined by asymptotic

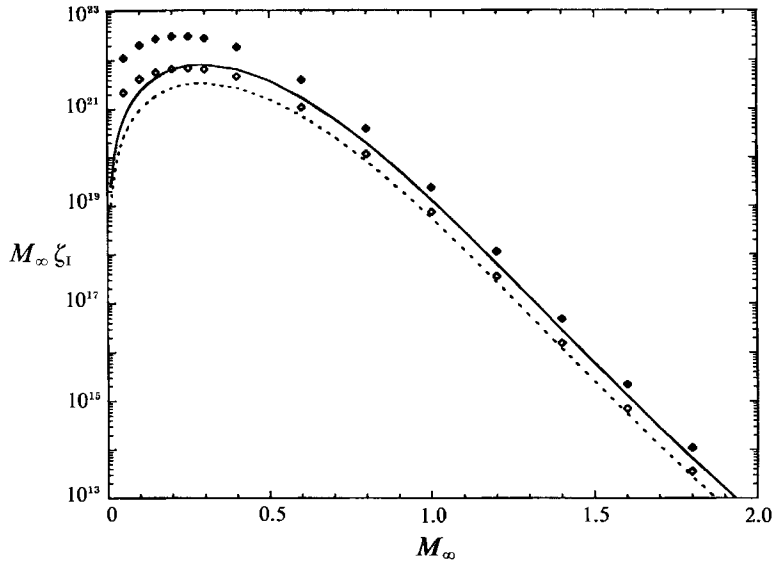

FIGURE 5. Log plot of the ignition distance, obtained both numerically and asymptotically, as a function of the free-stream Mach number for the adiabatic wall case: ——, asymptotic results with non-similar terms; – – –, asymptotic results with local-similarity assumption; ◆, numerical results with non-similar terms; ◇, numerical results with local-similarity assumption.

analysis and by numerical computation, for both the non-similar and locally similar cases. The agreement is seen to be quite good except for very small Mach numbers. This divergence of the solutions arises because, as can be seen from (21), our asymptotic analysis breaks down when $\mu \sim O(\epsilon^{\frac{1}{2}})$. For such small values of viscous heating, the frozen flow field has a uniform temperature distribution to first approximation. Consequently, effects of the reaction rate term will be felt throughout the entire domain $0 \leqslant \xi \leqslant 1$. Thus if we rescale the problem with $\mu = \tilde{\mu}\epsilon^{\frac{1}{2}}$, it is necessary to consider the full convective–diffusive–reactive equations in the entire flow field. Therefore, when $\mu \ll 1$, the full numerical treatment discussed in §3 is appropriate, although such small magnitudes of viscous heating are not the primary concern of the present study.

It is also noteworthy that the ignition distance passes through a maximum as M_∞ is increased through a critical value. This implies that the effect of viscous heating is not appreciable when the Mach number is very small, so that, as the flow velocity increases, ignition is delayed to a point further downstream. As the Mach number of the flow is increased further, however, viscous dissipation generates enough heat to cause a rapid rise in the reaction rate, thereby resulting in shorter ignition distances. Figure 5 illustrates that an $O(1)$ change in M_∞ results in a change of several orders of magnitude in x_I.

The above behaviour can be further demonstrated by noting the relation

$$x_I \sim M_\infty^2 T_\infty T_c^{\frac{1}{2}} \exp(T_a/T_c),$$

from (40), where $T_c = T_\infty[1+\frac{1}{2}(\gamma-1)M_\infty^2]$, so that the extremely sensitive nature of the ignition distance to changes in Mach number is seen to be due to the exponential dependence on M_∞^2. We also note that the ignition distance has an exponential dependence on the bulk flow temperature, T_∞. However, variations of x_I with T_∞ will be less dramatic than variations with bulk flow velocity since T_c depends only linearly on T_∞.

Finally, we note that the extremely large values of ζ_I that are obtained in this and subsequent cases (see figures 5, 6 and 8) are a consequence of the exponential dependence of ζ_I on the activation energy, T_a, as can be seen from (40). The actual ignition distance, x_I, takes on more modest values since it is inversely proportional to the pre-exponential factor, B (see (7)), which is assumed to be of the same order of magnitude as $\exp(T_a/T_c)$. Although it is possible to normalize $M_\infty \zeta_I$ with a large reference value, say $\exp(T_a/T_c)$, to present results with values representative of the order of magnitude of x_I, we choose not to do so since the characteristic temperature, T_c, is a function of Mach number. Our intent in each of these figures is to demonstrate the variation of ignition distance with Mach number, for a given mixture with a fixed pre-exponential factor. The actual magnitude of the ignition distance for a specific Mach number can be readily determined through the use of (7).

4.2. *Isothermal wall*

We now consider the ignition characteristics of boundary-layer flows in which the wall temperature is held constant. As discussed in §2 we should expect very different behaviour depending on whether α is greater or less than zero, since the maximum value of the frozen temperature profile shifts from the wall to a location inside the boundary layer as α is decreased below zero. We shall first analyse the situation with $\alpha > 0$ for which external heating from the wall is the dominant source for ignition. Following that, we consider $\alpha < 0$ for which viscous dissipation mainly provides the heat source for ignition. Both of these analyses break down as $|\alpha| \to 0$, i.e. when the frozen temperature profile becomes nearly adiabatic at the wall. Thus, in order to construct valid solutions over the entire range of Mach number, we shall also analyse this intermediate regime in §4.2.3 after rescaling α to be $O(\epsilon^{\frac{1}{2}})$.

4.2.1. *The subadiabatic wall case:* $\alpha > 0$

As shown in §2, the solution for the frozen temperature in this case is given by

$$T_f = T_w - \alpha\xi - \mu\xi^2, \tag{42}$$

which attains a maximum value T_w at the wall. Thus, as for the adiabatic case, we expect a thin reaction zone to be located near $\xi = 0$. The frozen profile (42) also suggests that the appropriate inner stretched coordinate is $X = \alpha\xi/\epsilon$, since the profile varies linearly with ξ within a narrow region near the wall. Note that the reaction zone is an order of magnitude smaller than that for the adiabatic wall. This is because the frozen temperature profile (42) for the present case drops off more rapidly as we move away from the wall, thereby freezing the reaction at a shorter distance from the wall.

We seek an inner solution of the form

$$T_{in}(X, \zeta) = T_f(X) + \epsilon\theta_0(X, \zeta) + O(\epsilon^2), \tag{43}$$

and after substituting this expansion into (17), the inner structure equation to leading order becomes

$$\frac{\partial^2\theta_0}{\partial X^2} = -\tfrac{1}{2}\Delta_{sub}\exp(\theta_0 - X), \tag{44}$$

where

$$\Delta_{sub} = \frac{2\epsilon\zeta}{[\alpha f''(0)]^2} Y_{O\infty}^p T_w^{r-p-q+1} \exp(-T_a/T_w). \tag{45}$$

The boundary condition at the wall, as well as a matching condition at $X \to \infty$, are given by

$$\theta_0(0, \zeta) = 0, \quad (\partial\theta_0/\partial X)(\infty, \zeta) = 0, \tag{46}$$

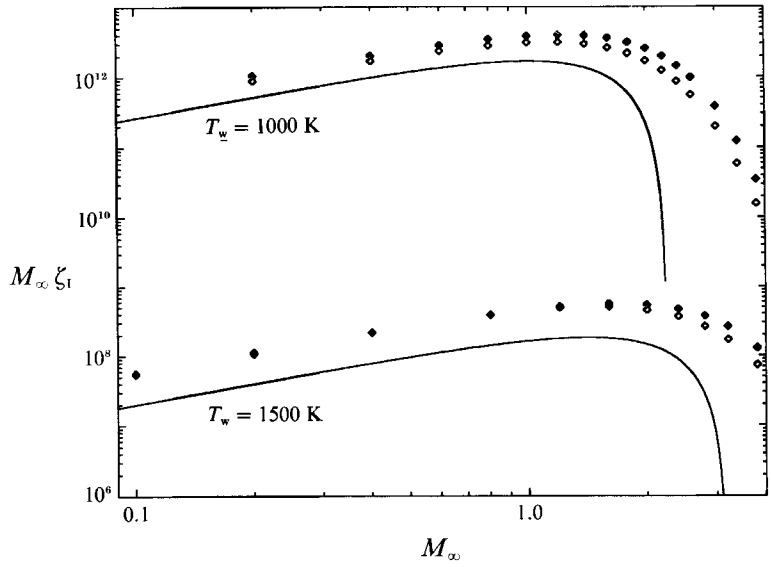

FIGURE 6. Log-log plot of the predicted ignition distance as a function of the free-stream Mach number for the hot-wall case. Curves are drawn for two different values of wall temperature: ——, asymptotic results; ◆, numerical results with non-similar terms; ◇, numerical results with local-similarity assumption.

where the latter condition is obtained by matching to the outer solution, which is expanded as $T_{\text{out}}(\xi, \zeta) = T_f(\xi) + \epsilon\Phi_0(\xi, \zeta) + O(\epsilon^2)$. These structure equations are identical to those studied by Law & Law (1979) for the related problem of subsonic boundary-layer ignition over a hot plate. The only modification is the appearance of the parameter α in Δ_{sub}, which represents the combined heat source due to the hot wall and the viscous heating effects (Ju & Niioka 1991). Equations (44)–(46) have been solved (Law 1978) and it was shown that no steady solutions exist for values of Δ_{sub} greater than unity. This critical state, $\Delta_{\text{sub}} = 1$, is the ignition point, and it was shown (Law 1978) to be consistent with the adiabaticity condition, or the van't Hoff criterion, which states that the onset of the self-sustaining reaction in the reactive medium occurs when the heat flux at the hot wall vanishes identically (Alkidas & Durbetaki 1973). From (45) we now find the ignition distance to be

$$\zeta_I = \frac{[\alpha f''(0)]^2}{2\epsilon Y_{O\infty}^p T_w^{r-p-q+1}} \exp(T_a/T_w). \tag{47}$$

In figure 6 we have plotted $M_\infty \zeta_I$ as a function of M_∞ as determined both numerically and from (47) for two different wall temperatures. Similar to the result in §4.1, each curve is seen to increase with M_∞ initially, a maximum value is reached and then the curve decreases. This is readily observed from the analytical result (47), which provides the explicit dependence of the ignition distance on the Mach number. Since $M_\infty \zeta_I \sim \mu^{\frac{1}{2}}(\beta - \mu)^2$, the maximum ignition point is easily calculated to occur when $\mu = \frac{1}{5}\beta$, or $M_\infty = \{2(T_w/T_\infty - 1)/[5(\gamma - 1)]\}^{\frac{1}{2}}$. For small values of M_∞, the viscous heating effect is small compared to the hot-wall effect such that the ignition point is swept further downstream in a manner proportional to the velocity. As we continue to increase the velocity, more heat is generated then can be swept away and this results in a decrease in the ignition distance. For this range of Mach number, the kinetic energy of the high-speed flow can be utilized to enhance the ignitibility of the mixture. Further increase in M_∞ eventually results in a breakdown of our analysis

when $\alpha \to 0$, i.e. when the heat generated by viscous dissipation becomes comparable to that generated by the hot wall.

Equation (47) also reveals the explicit dependence of the ignition distance on T_w, and figure 6 illustrates how an increase in T_w results in a shorter ignition distance. After each curve passes through its maximum point, we observe sharper drops in $M_\infty \zeta_I$ for smaller values of T_w. This implies that, for this range of M_∞, the ignition distance can be made less sensitive to Mach number variations by increasing the wall temperature.

Note that it was not necessary to solve the outer equation to determine ζ_I in this case since, as seen from the matching condition (46), there is no heat transfer between the inner and outer zones up to $O(\epsilon)$. Consequently, the effect of non-similarity in the outer frozen flow is minimized in the situation.

4.2.2. *The superadiabatic wall case:* $\alpha < 0$

When $\alpha < 0$, heat is transferred toward the wall and viscous dissipation is the energy source that induces ignition. The frozen temperature profile is again given by (42), but now the maximum value of $T_c = T_w + \alpha^2/4\mu$ is attained at $\xi_c = -\alpha/2\mu$. Thus we anticipate that ignition will occur inside the supersonic boundary layer at a distance ξ_c away from the wall. We first consider $\alpha = O(1)$ for which the structure of the boundary layer consists of two frozen outer zones, $0 < \xi < \xi_c$ and $\xi_c < \xi < 1$, of $O(1)$ length separated by a diffusive–reactive inner zone of thickness $O(\epsilon^{\frac{1}{3}})$ at $\xi = \xi_c$. We note that as $\alpha \to 0$ the ignition distance approaches the wall, and the present analysis breaks down. In §4.2.3 we will treat the intermediate regime for which $|\alpha| = O(\epsilon^{\frac{1}{3}})$.

In the reaction zone, the appropriate stretched inner coordinate is given by $Z = \mu^{\frac{1}{3}}(\xi - \xi_c)/\epsilon^{\frac{1}{3}}$ and we seek solutions of the form

$$T_{in}(Z, \zeta) = T_f(Z) + \epsilon\theta_0(Z, \zeta) + \epsilon^{\frac{2}{3}}\theta_1(Z, \zeta) + O(\epsilon^2). \tag{48}$$

After substituting the above expansions into equations (17)–(19*b*), we obtain a system of equations to be solved recursively at each order in ϵ. As for the adiabatic wall problem, when the magnitude of the Damköhler number is chosen such that the reaction term balances the leading-order diffusion term, then the structure equations do not possess a solution. Thus again, the ignition distance is overestimated, and it is necessary to rescale the Damköhler number as

$$\tilde{\Delta}_{sup} = \frac{1}{\epsilon^{\frac{1}{3}}} \frac{\zeta}{\mu[f''(\eta_c)]^2} Y_{O\infty}^p T_c^{r-p-q+1} \exp(-T_a/T_c), \tag{49}$$

where η_c is defined by $f'(\eta_c) = \xi_c$. With this scaling (49), the structure equations at the first two orders are

$$\partial^2\theta_0/\partial Z^2 = 0, \tag{50}$$

$$\partial^2\theta_1/\partial Z^2 = -\tilde{\Delta}_{sup} \exp(\theta_0 - Z^2), \tag{51}$$

and solutions to these equations must satisfy two boundary conditions which are found by matching to the outer solutions at $Z \to \pm\infty$. At leading order, we require that solutions be bounded as $Z \to \pm\infty$, and it follows from (50) that θ_0 must be a function of ζ only.

In the outer frozen flow regions on either side of the reaction zone, the temperature field is expanded as

$$T_{out}^{\pm}(\xi, \zeta) = T_f(\xi) + \epsilon\Phi_0^{\pm}(\xi, \zeta) + O(\epsilon^{\frac{2}{3}}), \tag{52}$$

where the leading-order temperature perturbation is continuous across the reaction zone, i.e.

$$\Phi_0^+(\xi_c, \zeta) = \Phi_0^-(\xi_c, \zeta) = \theta_0(\zeta), \tag{53}$$

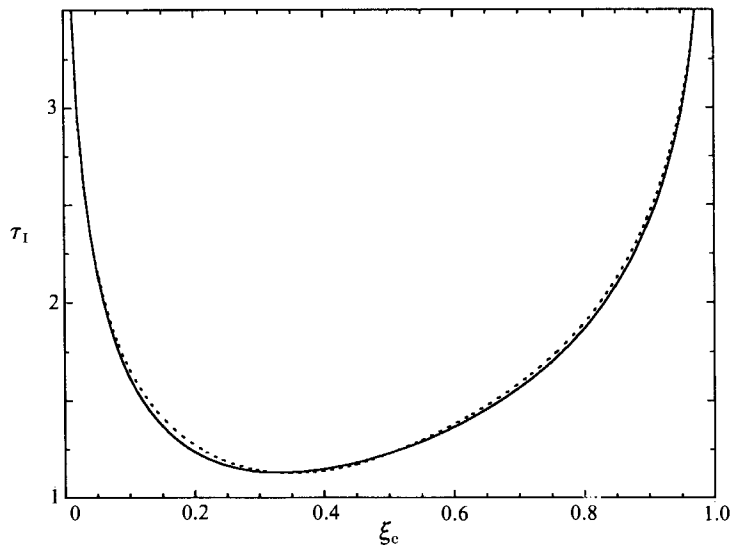

FIGURE 7. Functional relation between the streamwise, τ_I, and transverse, ξ_c, location of ignition for the viscous heating case: ——, numerical result; – – –, fitted curve given by the correlation function (58).

and matching the gradients to the solution of (51) yields

$$\frac{\partial \Phi_0^{\pm}}{\partial \xi}(\xi_c, \zeta) = \mu^{\frac{1}{2}} \frac{\partial \theta_1^{\pm}}{\partial Z} = \mp \frac{(\pi\mu)^{\frac{1}{2}}}{2} \tilde{A}_{\sup} \exp[\Phi_0(\xi_c, \zeta)] + C(\zeta), \quad Z \to \pm\infty, \tag{54}$$

where the function $C(\zeta)$, which arises through one integration of (51), is as yet unknown. It is convenient to introduce the variable $\tau = \ln[(\pi\mu)^{\frac{1}{2}} \tilde{A}_{\sup}]$, so that when (52) is inserted into (17)–(19*b*) the equation for the leading-order temperature perturbation becomes

$$\frac{\partial^2 \Phi_0^{\pm}}{\partial \xi^2} - \frac{2\xi}{[f''(\eta)]^2} \frac{\partial \Phi_0^{\pm}}{\partial \tau} = 0, \quad \xi \neq \xi_c, \tag{55}$$

subject to the boundary conditions

$$\Phi_0^-(0, \tau) = \Phi_0^+(1, \tau) = \Phi_0^{\pm}(\xi, -\infty) = 0. \tag{56}$$

Furthermore, we can eliminate $C(\zeta)$ from (54) to obtain the jump condition at $\xi = \xi_c$

$$\left[\frac{\partial \Phi_0}{\partial \xi}\right]_-^+ = \frac{\partial \Phi_0^+}{\partial \xi}(\xi_c, \tau) - \frac{\partial \Phi_0^-}{\partial \xi}(\xi_c, \tau) = -\exp[\Phi_0(\xi_c, \tau) + \tau], \tag{57}$$

which relates the gradients on either side of ξ_c in terms of $\Phi_0(\xi_c, \tau)$. The appearance of the streamwise convection term in (55) again represents the non-similar effects in both outer flow fields. A similar structure problem has also been independently obtained by Grosch & Jackson (1991) in the related problem of ignition in a compressible mixing layer. Our system (55)–(57), containing the single parameter ξ_c which varies from 0 to 1, was solved numerically, and figure 7 shows the distance τ_I at which the temperature perturbation blows up as a function of the parameter ξ_c. A useful correlation for this curve, which is accurate to within a few percent error, is given by

$$\tau_I(\xi_c) = \tau_I(0.5) - 2\ln[f''(\eta_c)/f''(1.092)] + 0.448[|\ln(\xi_c/0.5)|^{1.36} - |\ln[(1-\xi_c)/0.5]|^{1.33}], \tag{58}$$

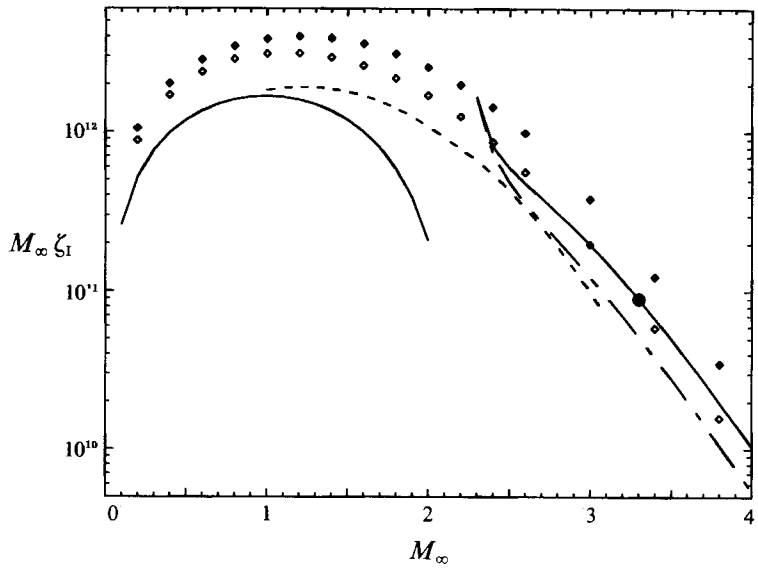

FIGURE 8. Log plot of the predicted ignition distance as a function of the free-stream Mach number for the isothermal wall. Curves illustrate how asymptotic solutions in each regime match together to provide results over the entire range of M_∞: ——, asymptotic results for subadiabatic wall case; —●—, asymptotic results for superadiabatic wall case with non-similar terms; —·—, asymptotic results for superadiabatic wall with local-similarity assumption; – – –, asymptotic results for intermediate case; ◆, numerical results with non-similar terms; ◇, numerical results with local-similarity assumption.

where $f'(1.092) = 0.5$ and $\tau_I(0.5) \approx 1.230$. By using (58) and the definition of τ, we now find the final solution for the ignition distance to be

$$\zeta_I = \exp[\tau_I(\xi_c)]\left(\frac{\mu\epsilon}{\pi}\right)^{\frac{1}{3}} \frac{[f''(\eta_c)]^2}{Y_{O\infty}^p T_c^{r-p-q+1}} \exp(T_a/T_c). \tag{59}$$

In deriving this expression, we remark that non-similar effects were accounted for in the two frozen regions on either side of the reaction zone. Asymptotic analysis enabled us to simplify the original problem to the reduced system (55)–(57) for the temperature perturbation across a discontinuity. Nevertheless, this reduced problem consists of a partial differential equation with a nonlinear boundary condition, which required numerical treatment.

As discussed in our study of the adiabatic wall, §4.1, if the local-similarity assumption is made in the outer zone, then it is possible to construct analytical solutions which possess a turning point at

$$\tau_I(\xi_c) = -1 - \ln[\xi_c(1-\xi_c)]. \tag{60}$$

This expression then replaces the correlation (58), but again the ignition distance is underestimated by a factor of approximately two. It is easy to verify from (60) that, when the local-similarity approximation is made, τ_I achieves its minimum value at $\xi_c = \frac{1}{2}$, i.e. when $T_w = T_\infty$. However, as illustrated in figure 7, non-similar effects cause this minimum to shift into the region $\xi_c < \frac{1}{2}$ for which $T_w > T_\infty$.

In figure 8 we compare the ignition distances found asymptotically in §4.2.1 and §4.2.2, for α greater and less than zero respectively, with the numerical results of §3. For the viscous heating case, $\alpha < 0$, results when making the local-similarity assumption are also provided and are denoted by the dotted curve. In this

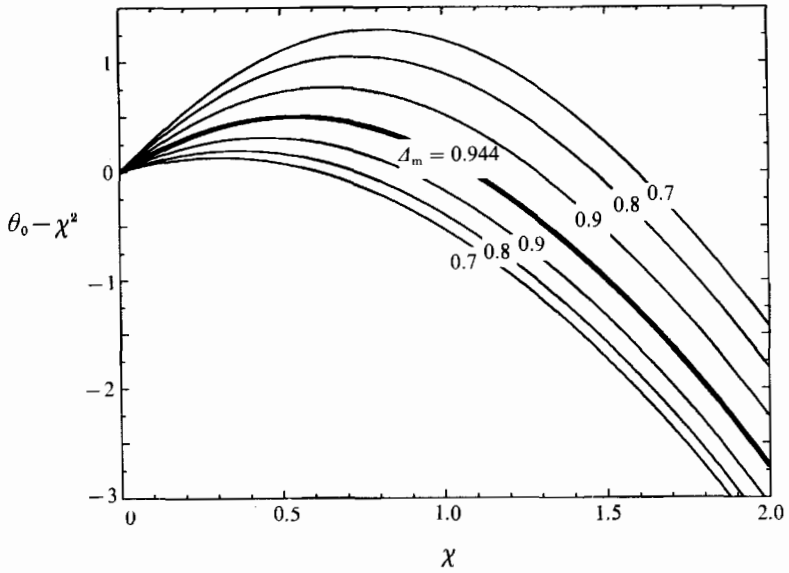

FIGURE 9. The solution of (62)–(64) for the intermediate regime when $\Gamma = 0$.

calculation, the wall and ambient temperatures are held constant at 1000 K and 500 K respectively, while the Mach number is varied. Both asymptotic analyses are seen to break down as $|\alpha| \to 0$, which corresponds to $M_\infty \approx 2.24$ for the parameter values used here. In order to complete our analysis and to provide explicit results over the entire range of M_∞, we now consider small values of $|\alpha|$.

4.2.3. *The nearly adiabatic wall (intermediate) case:* $|\alpha| \ll 1$

Based on previous discussions, our analyses are no longer valid when the magnitude of α becomes $O(\epsilon^{\frac{1}{2}})$. Thus we rescale α as $\alpha = \epsilon^{\frac{1}{2}}\tilde{\alpha}$, introduce the stretched coordinate $\chi = \mu^{\frac{1}{2}}\xi/\epsilon^{\frac{1}{2}}$, and seek solutions for the inner temperature profile as

$$\begin{aligned} T_{\text{in}}(\chi, \zeta) &= T_{\text{f}}(\chi) + \epsilon\theta_0(\chi, \zeta) + O(\epsilon^{\frac{3}{2}}) \\ &= T_{\text{w}} + \epsilon[\theta_0 - (\chi^2 + \Gamma\chi)] + O(\epsilon^{\frac{3}{2}}), \end{aligned} \tag{61}$$

where $\Gamma = \tilde{\alpha}/\mu^{\frac{1}{2}}$. To leading order, the inner structure equation is given by

$$\partial^2\theta_0/\partial\chi^2 = -\Delta_{\text{m}} \exp(\theta_0 - \chi^2 - \Gamma\chi), \tag{62}$$

where

$$\Delta_{\text{m}} = \frac{\zeta}{\mu[f''(0)]^2} Y_{\text{O}\infty}^p T_{\text{w}}^{r-p-q+1} \exp(-T_{\text{a}}/T_{\text{w}}), \tag{63}$$

and the boundary and matching conditions are

$$\theta_0(0, \zeta) = 0, \quad (\partial\theta_0/\partial\chi)(\infty, \zeta) = 0. \tag{64}$$

The reactive–diffusive equation (62) together with boundary conditions (64) can be solved independently of the outer frozen zone structure. Thus, the non-similar nature of the outer frozen flow does not greatly affect the ignition characteristics. Although a first integration of (62) can be performed, no explicit analytical solutions to (62)–(64) could be found and so the system was solved numerically in order to obtain the critical ignition distance as a function of Γ. In figure 9 we have set $\Gamma = 0$ and plotted the quantity $\theta_0 - \chi^2$, which represents the actual temperature profile near the

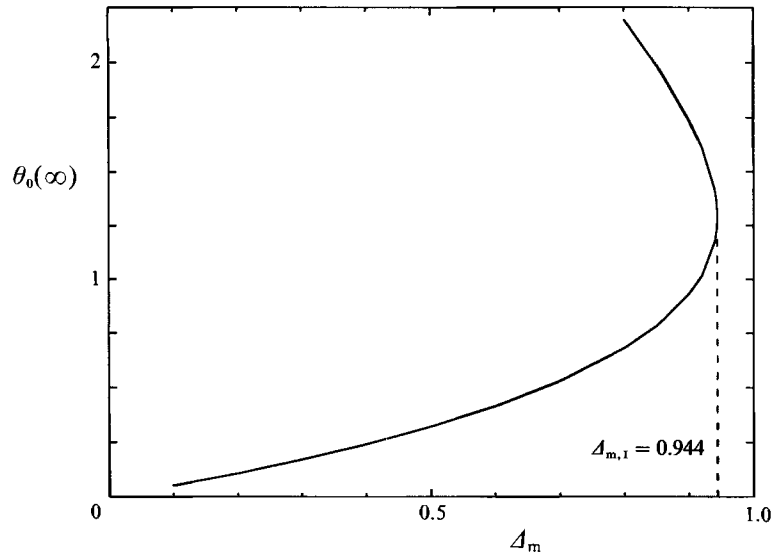

FIGURE 10. The maximum temperature perturbation $\theta_0(\infty)$ versus system Damköhler number Δ_m for the intermediate regime, illustrating turning point behaviour.

hot wall, for various values of the parameter Δ_m. Multiple solutions are found to exist up to the critical value of $\Delta_m = 0.944$, beyond which there are no solutions. This turning point behaviour is clearly illustrated in figure 10, where the maximum value of θ_0 is plotted versus Δ_m. The critical value, which we denote by $\Delta_{m,I}$, then provides the ignition criterion.

The fact that the ignition point in this problem is given by the turning point of the maximum temperature perturbation is expected since equations (62)–(64) are locally similar. It should also be noted from figure 9 that, at the criticality point ($\Delta_{m,I} = 0.944$), the temperature gradient is superadiabatic at the wall. This contrasts with the result of the subadiabatic wall case in which the criticality criterion and the adiabaticity criterion were found to be equivalent. Recall that a similar situation was found to hold for the adiabatic wall and the superadiabatic isothermal wall cases when the locally similar approximation was made. In both cases, ignition was determined from the criticality condition, while the adiabaticity criterion was not the appropriate condition to predict the onset of reaction. Only when the inert temperature profile varies linearly within the thin reaction layer, such as in the hot-wall ignition problem, are the two criteria equivalent.

The objective of this analysis is to determine $\Delta_{m,I}$, and since (62) has an additional parameter, Γ, the resulting ignition Damköhler number must be a function of Γ. Although no explicit expression can be found for $\Delta_{m,I}(\Gamma)$, a useful correlation for this curve, accurate to within a few percent, is given by

$$\Delta_{m,I}(\Gamma) = \begin{cases} 0.944\exp[0.85\Gamma - 0.17\Gamma^2] & \text{for} \quad \Gamma \leqslant 0, \\ 0.944 + 0.80\Gamma + 0.41\Gamma^2 & \text{for} \quad \Gamma \geqslant 0. \end{cases} \tag{65}$$

Equation (63) can now be used to determine the ignition distance as

$$\zeta_I = \Delta_{m,I}(\Gamma)\frac{\mu[f''(0)]^2}{Y_{O\infty}^p T_w^{r-p-q+1}}\exp(T_a/T_w), \tag{66}$$

and the result is plotted in figure 8 as the dashed curve. The solution for this narrow

range of Mach numbers bridges the gap between the solutions obtained earlier for values of α greater and less than zero. Thus we have succeeded in explicitly determining the ignition distance over the entire range of Mach numbers for the problem of supersonic boundary-layer ignition over an isothermal wall.

It is also of interest to note that the ignition characteristics for the intermediate regime studied in this section are markedly different from those for the adiabatic wall despite the fact that they have the same leading-order inert temperature profile, with T_c replaced with T_w. This illustrates the significant effect that the wall conditions can have on the ignition delay in supersonic boundary layer flows. For the isothermal wall with $|\alpha| \ll 1$, although the frozen profile is adiabatic to leading order, the reaction-zone temperature perturbation is suppressed at the wall. This causes the reaction to initiate at a greater distance from the wall than when adiabatic conditions are applied. Consequently, the evolving hot kernel loses heat to both directions at the point of maximum temperature, thereby resulting in a longer ignition distance. Indeed, if we compare the result (66) of the present section to (40) of §4.1, we observe that the ignition distance for the adiabatic wall is $O(\epsilon^{\frac{1}{2}})$ smaller than that of the isothermal wall.

5. Concluding remarks

The thermal ignition of a premixed combustible within a supersonic flat-plate boundary layer has been studied asymptotically by exploiting the realistic limit of large activation energy. In particular, we have derived explicit expressions for the minimum ignition distance along the streamwise coordinate for both adiabatic and isothermal walls. These expressions provide the necessary information to predict ignition events, and also reveal the effects of the various system parameters on the ignition distance. One parameter of particular importance is the viscous heating term, μ, that appears in the energy equation for supersonic flows. It was shown that the ignition characteristics of boundary layer flows depends significantly on whether this parameter is greater or less than the inviscid heat transfer parameter, β. In particular, when $\beta > \mu$, ignition was shown to occur when the heat transfer at the hot wall vanished identically. On the other hand, when $\mu > \beta$, viscous heating is the dominant mechanism for ignition, and the frozen flow has a temperature bulge at a finite distance from the wall so that the temperature profile is superadiabatic at the wall. For this case, as well as for the adiabatic wall case, non-similar effects are important and ignition is interpreted as the state at which the solution for the temperature perturbation blows up.

In general, the structure of a weakly reacting supersonic boundary layer was found to consist of an inner, locally similar, diffusive–reactive region near the point of maximum temperature and an outer diffusive–convective, generally non-similar region. Although the reaction term vanishes to all algebraic orders in the outer layer, the frozen region becomes non-similar due to the heat transfer from the thin reactive layer. It was shown that, for the adiabatic wall and the isothermal wall with sufficiently large viscous heating, failure to include these non-similar effects results in an underestimation of the ignition distance by a factor of about two. For the hot-wall ignition problem, the driving mechanism for ignition is the heat transfer from the wall and the problem is basically the same as that for ignition in subsonic boundary layers. It was found that non-similar effects in the boundary layer are less important for this case because there is no heat transfer between the frozen and reaction zones to first approximation.

Although our results compare favourably to direct numerical solutions, the critical distance determined by numerical calculation is always found to exceed the asymptotic result. There are several factors that lead to the difference in these solutions. First, in the numerical study the ignition point was defined to be the location at which the actual temperature profile achieved thermal runaway, whereas in the asymptotic analysis ignition was determined from the behaviour of the temperature perturbation. Secondly, since the asymptotic analysis is valid for small values of the perturbation parameter ϵ, the results become more accurate as $\epsilon \to 0$. Indeed it can be shown that better agreement between the curves in figures 5 and 8 is observed for larger values of the activation energy or smaller values of the maximum inert temperature, both of which result in smaller values of ϵ. Thirdly, we note that reactant consumption is negligible in the asymptotic analysis, while these effects are fully accounted for in the numerical calculation. The ignition distances (40), (47), (59) and (66) are found to be inversely proportional to the mass fraction of each species, and thus consumption is expected to weaken the reaction rate and cause a longer delay before ignition. Effects of reactant consumption were considered by Liñán & Williams (1971, 1972, 1979) for the ignition of a solid with various external heat sources, and by Law & Law (1981) for subsonic boundary-layer ignition. These asymptotic analyses provide higher-order correction terms to the critical ignition time, and indeed it was shown that reactant consumption causes a delay in ignition.

Equation (7) can be used to write each of the expressions (40), (47), (59) and (66) for the ignition distances in terms of the original streamwise physical coordinate, x, in order to assess the effects of the various system parameters on the actual ignition distance, x_{I}. In particular, x_{I} is seen to vary in an Arrhenius manner with the maximum characteristic temperature, T_{c}, and it is proportional to the dissipation function, $(f'')^2$.

Finally, we remark that the present analysis is only concerned with events leading up to ignition. Once ignition occurs, a flame develops that propagates upstream and is stabilized at a location where the flame speed balances the flow speed. In the presence of a fully developed flame, the structure becomes much more complicated as the similar nature of the boundary layer needs to be re-examined and shock waves may also develop. A better understanding of such interesting phenomena requires further study.

This research has been supported by the Air Force Office of Scientific Research under the technical monitoring of Dr J. M. Tishkoff. The authors wish to thank Dr B. H. Chao for his many helpful comments regarding this work.

REFERENCES

Alkidas, A. & Durbetaki, P. 1973 Ignition of a gaseous mixture by a heated surface. *Combust. Sci. Tech.* **7**, 135.

Cheng, S. I. & Kovitz, A. A. 1957 Ignition in the laminar wake of a flat plate. *6th Symp. (Intl.) Combust.*, p. 418. Reinhold.

Cheng, S. I. & Kovitz, A. A. 1958 Mixing and chemical reaction in the laminar wake of a flat plate. *J. Fluid Mech.* **4**, 64.

Chung, P. M. 1965 Chemically reacting nonequilibrium boundary layers. In *Advances in Heat Transfer*, vol. 2, pp. 109–270. Academic.

Dooley, D. A. 1957 Ignition in the laminar boundary layer of a heated plate. *1957 Heat Transfer and Fluid Mech. Inst.*, pp. 321–342. Stanford University Press

FIGUEIRA DA SILVA, L. F., DESHAIES, B. & CHAMPION, M. 1992 A numerical study of hydrogen-air combustion within a supersonic boundary layer. *AIAA Paper* 92-0338.

GROSCH, C. E. & JACKSON, T. L. 1991 Ignition and structure of a laminar diffusion flame in a compressible mixing layer with finite rate chemistry. *Phys. Fluids* A3, 3087.

HUMPHREY, J. W. & SOBOTA, T. H. 1991 Beyond rockets: the scramaccelerator. *Aerospace America*, June 1991, p. 18.

JACKSON, T. L. & HUSSAINI, M. Y. 1988 An asymptotic analysis of supersonic reacting mixing layers. *Combust. Sci. Tech.* **57**, 129.

JU, Y. & NIIOKA, T. 1991 *Proc. 29th Japanese Symp. on Combustion*, Nos. 127 and 128. (In Japanese.)

LAW, C. K. 1978 On the stagnation-point ignition of a premixed combustible. *Intl. J. Heat Mass Transfer* **21**, 1363.

LAW, C. K. 1992 Mechanisms of flame stabilization in subsonic and supersonic flows. In *Major Research Topics in Combustion* (ed. Hussaini, Kumar, & Voight), pp. 201–236. Springer.

LAW, C. K. & LAW, H. K. 1979 Thermal-ignition analysis in boundary-layer flows. *J. Fluid Mech.* **92**, 97.

LAW, C. K. & LAW, H. K. 1981 Flat-plate ignition with reactant consumption. *Combust. Sci. Tech.* **25**, 1.

LIÑÁN, A. & CRESPO, A. 1976 An asymptotic analysis of unsteady diffusion flames for large activation energies. *Combust. Sci. Tech.* **14**, 95.

LIÑÁN, A. & WILLIAMS, F. A. 1971 Theory of ignition of a reactive solid by constant energy flux. *Combust. Sci. Tech.* **3**, 91.

LIÑÁN, A. & WILLIAMS, F. A. 1972 Radiant ignition of a reactive solid with in-depth absorption. *Combust. Flame* **18**, 85.

LIÑÁN, A. & WILLIAMS, F. A. 1979 Ignition of a reactive solid exposed to a step in surface temperature. *SIAM J. Appl. Maths.* **36**, 587.

MARBLE, F. E. & ADAMSON, T. C. 1954 Ignition and combustion in a laminar mixing zone. *Jet Propulsion* **24**, 85.

SCHLICHTING, H. 1979 *Boundary Layer Theory*. McGraw-Hill.

SHARMA, O. P. & SIRIGNANO, W. A. 1970 On the ignition of a premixed fuel by a hot projectile. *Combust. Sci. Tech.* **1**, 481.

TREVIÑO, C. & MÉNDEZ, F. 1991 Asymptotic analysis of the ignition of hydrogen by a hot plate in a boundary layer flow. *Combust. Sci. Tech.* **78**, 197.

WALTRUP, P. J. 1986 Liquid fueled supersonic combustion ramjets: A research perspective of the past, present and future. *AIAA Paper* 86-0158.

WILLIAMS, F. A. 1985 *Combustion Theory*, 2nd edn. Benjamin Cummings.